Bell-inequality tests with entanglement between an atom and a coherent state in a cavity

Jinwoo Park,[1,2] Mark Saunders,[1,2,3] Yong-il Shin,[1] Kyungwon An,[1] and Hyunseok Jeong[1,2,*]

[1]*Department of Physics and Astronomy, Seoul National University, Seoul, 151-742, Korea*
[2]*Center for Macroscopic Quantum Control, Seoul National University, Seoul, 151-742, Korea*
[3]*Department of Education, University of Oxford, 15 Norham Gardens, Oxford, OX2 6PY United Kingdom*

We study Bell-inequality tests with entanglement between a coherent-state field in a cavity and a two-level atom. In order to detect the cavity field for such a test, photon on-off measurements and photon number parity measurements, respectively, are investigated. When photon on-off measurements are used, at least 50% of detection efficiency is required to demonstrate violation of the Bell inequality. Photon number parity measurements for the cavity field can be effectively performed using ancillary atoms and an atomic detector, which leads to large degrees of Bell violations up to Cirel'son's bound. We also analyze decoherence effects in both field and atomic modes and discuss conditions required to perform a Bell inequality test free from the locality loophole.

I. INTRODUCTION

Einstein, Podolsky, and Rosen (EPR) presented an argument known as the EPR paradox [1], which triggered the debate on quantum mechanics versus local realism. Bell's theorem [2] enables one to perform experiments in which failure of local realism is demonstrated by the violation of Bell's inequality. Various versions of Bell's inequality have been developed, including Clauser, Horne, Shimony, and Holt (CHSH)'s [3], and a substantial amount of experimental effort has been devoted to the successful demonstration of violation of Bell's inequality. So far, many experiments have been performed to show violation of Bell-type inequalities, and most physicists now seem to believe that local realism can be violated.

On the other hand, all the experiments performed to date are subject to some loopholes, so the experimental data can still be explained somehow based on a classical (often impellent) argument. Experiments using optical fields [4–7] typically suffer from the "detection loophole" [8], and recent experiments using atomic states [9,10] with the maximum separation of ∼1 m [10] suffer from the "locality loophole" [11]. While most of Bell inequality tests have been performed using entangled optical fields [4–7], it is an interesting possibility to explore Bell inequality tests using atom-field entanglement [12–16], particularly for a loophole-free test. In fact, there exist theoretical proposals for a loophole-free Bell inequality test using hybrid entanglement between atoms and photons [14,17,18] and relevant experimental efforts [10,15,19] have been reported.

In this paper, we study Bell inequality tests with an entangled state of a two-level atom and a coherent-state field. When the amplitude of the coherent state is large enough, such an entangled state is often called a "Schrödinger cat state" (e.g., in Ref. [20]) as an analogy of Schrödinger's paradox where entanglement between a microscopic atom and a classical object is illustrated [21]. Entanglement between atoms and coherent states has been experimentally demonstrated using cavities [22–24].

In our study, photon on-off measurements and photon number parity measurements, respectively, are employed in order to detect the cavity field. We find that when photon on-off measurements are used, at least 50% of detection efficiency is required to demonstrate violation of the Bell-CHSH inequality. One may effectively perform photon number parity measurements for the cavity field using ancillary probe atoms and an atomic detector so that nearly the maximum violation of the Bell-CHSH inequality can be achieved.

The remainder of this paper is organized as follows. In Sec. II, we briefly discuss the atom-field entanglement under consideration and review basic elements of Bell inequality tests in our framework. We then investigate the Bell-CHSH inequality with photon on-off measurements and parity measurements, respectively, in Sec. III. Section IV is devoted to the investigation of the Bell-CHSH inequality test using indirect measurements within a "circular Rydberg atom-microwave cavity" system. In Sec. V, we analyze decoherence effects in both field and atomic modes. This analysis enables us to provide quantitative information on the requirements to perform a loophole-free Bell test. We conclude with final remarks in Sec. VI.

II. BASIC ELEMENTS FOR BELL INEQUALITY TESTS

We are interested in testing the Bell-CHSH inequality with an atom-field entangled state:

$$|\Psi\rangle_{AC} = \frac{1}{\sqrt{2}}(|e\rangle_A|\alpha\rangle_C + |g\rangle_A|-\alpha\rangle_C), \qquad (1)$$

where $|e\rangle_A$ ($|g\rangle_A$) is the excited (ground) state for the atomic mode A and $|\pm\alpha\rangle_C$ are coherent states of amplitudes $\pm\alpha$ for the field mode C. States (1) for reasonably large values of α are considered entanglement between a microscopic system and a classical system [20,25–27]. There have been studies on Bell inequality tests with this type of entangled state [20] and similar states such as entanglement between an atom and a single photon [12–15] and entanglement between coherent states [25,28–36]. Experimental demonstration of state (1) has been performed using a system composed of a circular Rydberg atom and a microwave cavity field [22–24].

_____
*h.jeong37@gmail.com

In order to test a Bell type inequality, a bipartite entangled state should be shared by two separate parties. After sharing the entangled state, each of the two parties may locally perform appropriate unitary operations and dichotomic measurements. Violation of the Bell-CHSH inequality can be obtained by choosing certain values for the parameters of the unitary operations. The correlation function is defined as the expectation value of the joint measurement

$$E(\zeta,\beta) = \langle \hat{E}_A(\zeta) \otimes \hat{E}_C(\beta) \rangle, \qquad (2)$$

where $\hat{E}_A(\zeta) = \hat{U}_A^{\dagger}(\zeta)\hat{\Gamma}_A\hat{U}_A(\zeta)$ is a dichotomic measurement $\hat{\Gamma}_A$ combined with unitary operation $\hat{U}_A(\zeta)$ parameterized by ζ and $\hat{E}_C(\beta)$ can be defined accordingly. The Bell function $\mathcal{B}$ is then defined as

$$\mathcal{B} = E(\zeta,\beta) + E(\zeta',\beta) + E(\zeta,\beta') - E(\zeta',\beta'), \qquad (3)$$

which should obey the inequality forced by local realism, i.e., $|\mathcal{B}| \leqslant 2$. The maximum bound for the absolute value of the Bell function is $2\sqrt{2}$, known as Cirel'son's bound [37].

An atomic dichotomic measurement can be represented by a 2×2 matrix,

$$\hat{\Gamma} = \begin{pmatrix} 1 & 0 \\ 0 & -1 \end{pmatrix}, \qquad (4)$$

where we choose the basis as $\{|e\rangle, |g\rangle\}$. We define the displaced dichotomic measurement $\hat{\Gamma}(\zeta)$ with the atomic displacement operator $\hat{D}(\zeta)$ as

$$\hat{\Gamma}(\zeta) = \hat{D}(\zeta)\hat{\Gamma}\hat{D}^{\dagger}(\zeta) \qquad (5)$$

with

$$\hat{D}(\zeta) = \exp\left[\zeta\hat{\sigma}_+ - \zeta^*\hat{\sigma}_-\right] = \begin{pmatrix} \cos|\zeta| & \frac{\zeta}{|\zeta|}\sin|\zeta| \\ -\frac{\zeta^*}{|\zeta|}\sin|\zeta| & \cos|\zeta|, \end{pmatrix},$$
$$\zeta(\theta,\phi) = -\frac{\theta}{2}e^{-i\phi}, \qquad (6)$$

and $0 \leqslant \theta \leqslant \pi$ and $0 \leqslant \phi \leqslant 2\pi$, where $\hat{\sigma}_{\pm}$ are the standard ladder operators in the two-dimensional Hilbert space. We note that $\hat{D}(\zeta)$ corresponds to a single qubit rotation for an atomic qubit and it can be achieved by applying a Ramsey pulse to the atom [38]. We consider measurement $\hat{\Gamma}(\zeta)$ for the atomic mode A throughout the paper, while some different measurement schemes are considered for the field mode C.

III. BELL-CHSH INEQUALITY TESTS WITH ATOM-FIELD ENTANGLEMENT

A. On-off measurement for field mode

We, first, investigate the Bell-CHSH inequality with photon on-off measurements and the displacement operator for the cavity field mode. The displaced on-off measurement for the field C is

$$\hat{\mathcal{O}}_C(\beta) = \hat{\mathcal{D}}_C(\beta)\left(\sum_{n=1}^{\infty}|n\rangle\langle n| - |0\rangle\langle 0|\right)\hat{\mathcal{D}}_C^{\dagger}(\beta), \qquad (7)$$

where $\hat{\mathcal{D}}_C(\beta) = \exp[\beta\hat{a}_C^{\dagger} - \beta^*\hat{a}_C]$ is the displacement operator with the field annihilation (creation) operator $\hat{a}_C$ ($\hat{a}_C^{\dagger}$) and β as the displacement parameter for field C.

We model a photodetector with efficiency η by a perfect photodetector together with a beam splitter of transmissivity $\sqrt{\eta}$ in front of it [39]. The signal field C is mixed with the vacuum state $|0\rangle_v$ at a beam splitter. The beam splitter operator between modes C and v is $\hat{B}_{Cv} = \exp[(\cos^{-1}\sqrt{\eta})(\hat{a}_C^{\dagger}\hat{a}_v - \hat{a}_C\hat{a}_v^{\dagger})/2]$ [40], where $\hat{a}_v$ ($\hat{a}_v^{\dagger}$) is the field annihilation (creation) operator for the ancilla mode v. After passing through the beam splitter, the atom-field entangled state $|\Psi\rangle_{AC}$ is changed to a mixed state as

$$\rho_{AC}^{\eta} = \text{Tr}_v[\hat{B}_{Cv}(|\Psi\rangle\langle\Psi|)_{AC} \otimes (|0\rangle\langle 0|)_v \hat{B}_{Cv}^{\dagger}]$$
$$= \frac{1}{2}\{|e\rangle\langle e| \otimes |\sqrt{\eta}\alpha\rangle\langle\sqrt{\eta}\alpha| + |g\rangle\langle g| \otimes |-\sqrt{\eta}\alpha\rangle\langle-\sqrt{\eta}\alpha|$$
$$+ e^{-2(1-\eta)|\alpha|^2}|e\rangle\langle g| \otimes |\sqrt{\eta}\alpha\rangle\langle-\sqrt{\eta}\alpha|$$
$$+ e^{-2(1-\eta)|\alpha|^2}|g\rangle\langle e| \otimes |-\sqrt{\eta}\alpha\rangle\langle\sqrt{\eta}\alpha|\}_{AC}. \qquad (8)$$

The correlation function with the photon detection efficiency η is the expectation value of $\hat{\Gamma}_A(\zeta) \otimes \hat{\mathcal{O}}_C(\beta)$ for state (8) as

$$E_{\mathcal{O}}(\zeta,\beta;\eta) = \text{Tr}[\rho_{AC}^{\eta}\hat{\Gamma}_A(\zeta) \otimes \hat{\mathcal{O}}_C(\beta)]$$
$$= -e^{-|\beta|^2-|\alpha|^2\eta-2|\alpha||\beta|\sqrt{\eta}\cos\Phi}\cos\frac{\theta}{2}$$
$$+ e^{-|\beta|^2-|\alpha|^2\eta+2|\alpha||\beta|\sqrt{\eta}\cos\Phi}\cos\frac{\theta}{2} \qquad (9)$$
$$+ e^{-2|\alpha|^2}\cos\phi\sin\frac{\theta}{2}$$
$$- 2e^{-2|\alpha|^2-|\beta|^2+|\alpha|^2\eta}\cos(\phi - 2|\alpha||\beta|$$
$$\times \sqrt{\eta}\sin\Phi)\sin\frac{\theta}{2},$$

where $\alpha = |\alpha|e^{i\Phi_\alpha}$, $\beta = |\beta|e^{i\Phi_\beta}$, and $\Phi = \Phi_\beta - \Phi_\alpha$ with real phase parameters Φ_α and Φ_β. The Bell function is immediately obtained using Eqs. (3) and (9).

Using the method of steepest descent [41], we numerically find optimized values, $|\mathcal{B}_{\mathcal{O}}|_{\max}$, i.e., absolute values of the Bell function maximized over variables ζ, ζ', β, and β'. We plot the results against amplitude $|\alpha|$ for various choices of the detection efficiency from $\eta = 0$ to $\eta = 1$ (from bottom to top), where η differs by 0.1 between closest curves in Fig. 1. Assuming a real positive value of α, we find that the optimizing conditions can also be obtained as

$$\zeta = \frac{\pi}{2}, \zeta' = 0, \beta = -\beta' = |\beta|, \qquad (10)$$

where $|\beta|$ satisfies

$$2|\beta|e^{2(\eta-1)|\alpha|^2} = e^{-2|\alpha||\beta|\sqrt{\eta}}(|\beta| + |\alpha|\sqrt{\eta})$$
$$- e^{2|\alpha||\beta|\sqrt{\eta}}(|\beta| - |\alpha|\sqrt{\eta}). \qquad (11)$$

As expected, the perfect detection efficiency, $\eta = 1$, gives the higher violation up to $|\mathcal{B}_{\mathcal{O}}|_{\max} \approx 2.61$ when $|\alpha| \approx 0.664$. A Bell violation of $|\mathcal{B}_{\mathcal{O}}|_{\max} \approx 2.39$ ($|\mathcal{B}_{\mathcal{O}}|_{\max} \approx 2.14$) is obtained for $\eta = 0.8$ ($\eta = 0.6$) when $|\alpha| \approx 0.673$ ($|\alpha| \approx 0.692$).

When $|\alpha| = 0$, no violation occurs because state (1) contains no entanglement. As $|\alpha|$ increases, the Bell violation becomes higher until $|\alpha| \sim 0.7$. However, as shown in Fig. 1, as $|\alpha|$ keeps increasing, the degree of the Bell violation decreases toward zero even though the state has larger entanglement. This result is due to the fact that when $|\alpha|$ is large, the probability of detecting the vacuum
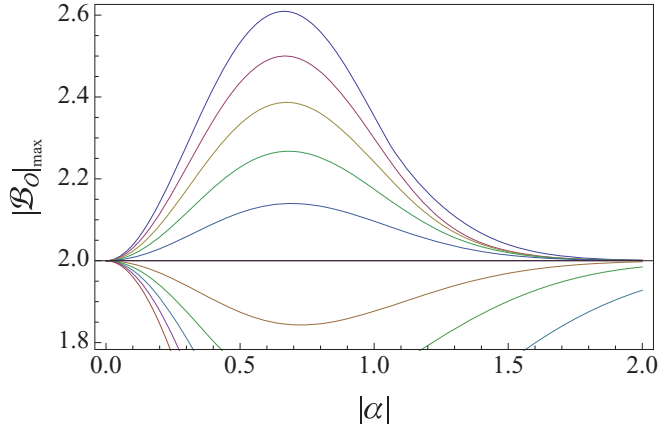
FIG. 1. (Color online) Numerically optimized values of Bell functions $\mathcal{B}_{\mathcal{O}}$ with displaced on-off measurements against amplitude α of state (1). The detection efficiency ranges in value from $\eta = 0$ (lower curve) to $\eta = 1$ (upper curve), with intervals of 0.1 shown by the family of curves. The horizontal line corresponds to the case of $\eta = 0.5$, which coincides with the classical limit of the Bell-CHSH inequality.

for the field mode diminishes. Obviously, if photon on-off detection excludes one of the two possible results, violation of the Bell-CHSH inequality will not occur regardless of the degree of entanglement. This is in agreement with a previous result in Ref. [30] where the Bell-CHSH inequality with entangled coherent states, $|\alpha\rangle|-\alpha\rangle - |-\alpha\rangle|\alpha\rangle$ (without normalization), was considered with on-off detection.

It should be noted that in Fig. 1, the Bell function for $\eta = 0.5$ overlaps with the horizontal line that indicates the classical limit 2. In fact, the photon detector efficiency should be higher than 0.5 in order to see a Bell violation as shown in Fig. 2(a). Figure 2(b) shows that the optimizing values of $|\alpha|$ are within the range of $0.66 < |\alpha| < 0.71$ for any of $\eta \geq 0.5$. We also note a previous result [16] that efficiency of 0.43 can be tolerated if a different type of Bell inequality [42] is used with a nonmaximally entangled state and a perfect atomic measurement.

B. Photon number parity measurement for field mode

We now consider the displaced photon number parity measurement for the field mode

$$\hat{\Pi}_C(\beta) = \hat{\mathcal{D}}_C(\beta)\bigg(\sum_{n=0}^{\infty} |2n\rangle\langle 2n|$$
$$- |2n+1\rangle\langle 2n+1|\bigg)\hat{\mathcal{D}}_C^{\dagger}(\beta). \quad (12)$$

Using Eq. (1) and the measurement operators defined above, it is straightforward to get

$$E_{\Pi}(\zeta,\beta) = \langle\hat{\Gamma}_A(\zeta) \otimes \hat{\Pi}_C(\beta)\rangle$$
$$= e^{-2|\beta|^2}\sin\theta\cos[4|\alpha||\beta|\sin\Phi - \phi]$$
$$+ e^{-2(|\alpha|^2+|\beta|^2)}\cos\theta\sinh[4|\alpha||\beta|\cos\Phi], \quad (13)$$

and the corresponding Bell function, $\mathcal{B}_{\Pi}$. We present the numerically optimized Bell function, $|\mathcal{B}_{\Pi}|_{max}$, against $|\alpha|$ in Fig. 3, where Bell violation occurs for any nonzero α.
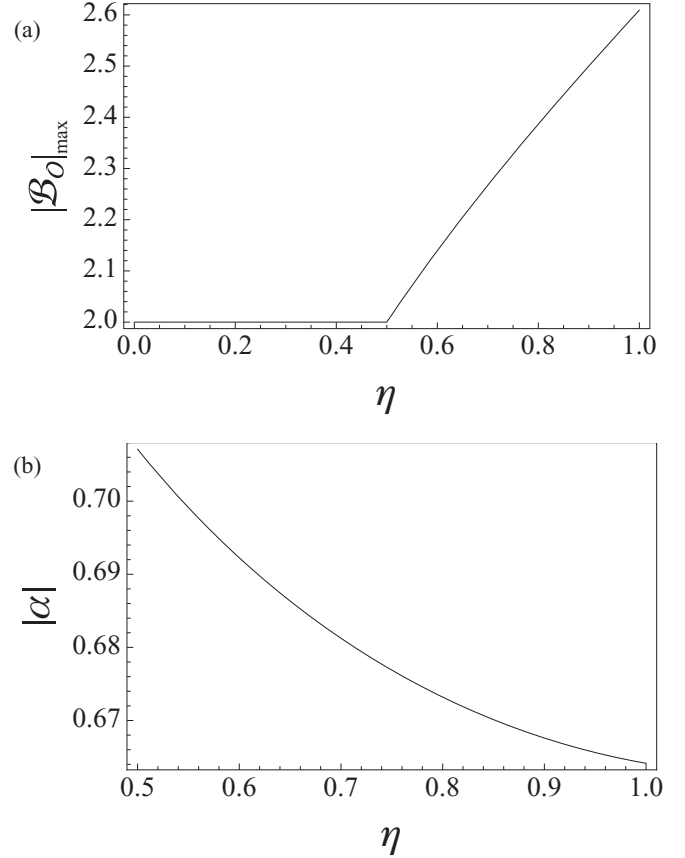

FIG. 2. (a) Numerically optimized values of Bell function $\mathcal{B}_{\mathcal{O}}$ with displaced on-off measurements against detection efficiency η. The local realistic bound, 2, is violated for $\eta \geq 0.5$. (b) Plot of optimizing values of $|\alpha|$ with respect to η.

Note that the atomic displacement operator corresponds to a single-qubit rotation for the atomic mode. It was argued that the field displacement plays a similar role to approximately rotate a coherent-state qubit [30]. If we restrict the atomic displacement parameters (ζ and ζ') to be real, our test becomes identical to the one in Ref. [20] and the result corresponds to the dashed curve in Fig. 3. However, it is not sufficient to reveal the maximal violation of the atom-field entangled state (1). In our numerical analysis, $\mathcal{B}_{\Pi}$ is optimized with respect to complex ζ, ζ', β, and β' that results in the solid curve in Fig. 3. Assuming that α is a real positive value, the optimizing conditions for $\mathcal{B}_{\Pi}$ are found as

$$\zeta = -\pi/4, \zeta' = i\pi/4, \beta = -\beta' = i|\beta|, \quad (14)$$

where $|\beta|$ satisfies

$$(|\alpha| - |\beta|)/(|\alpha| + |\beta|) = \tan 4|\alpha||\beta| \quad (15)$$

and is nearest to zero. As amplitude $|\alpha|$ increases, the degree of Bell violation rapidly gets larger up to Cirel'son's bound $2\sqrt{2}$.

IV. APPROACH USING INDIRECT MEASUREMENT

In this section, we discuss physical implementations of the Bell-CHSH inequality test using displaced parity measurements in a "circular Rydberg atom-microwave cavity"
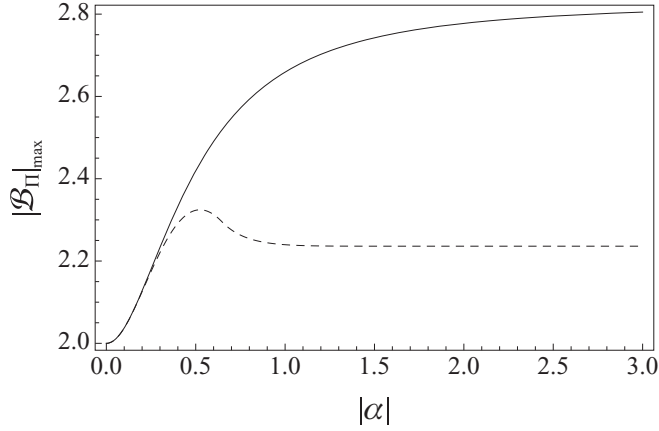
FIG. 3. Numerically optimized values of Bell function $\mathcal{B}_\Pi$ with displaced parity measurements against $|\alpha|$. The solid curve corresponds to the absolute values of the Bell function maximized over arbitrary ζ, ζ', β, and β', while the dashed curve corresponds to those values maximized over arbitrary β and β' but real ζ and ζ'.

FIG. 4. (Color online) Schematic of the proposal. The horizontal arrow is to describe the entangled state (1) generation (with R_A and C) and measurement for atom A. The vertical arrow depicts the indirect parity measurement of the cavity field using ancillary atom B.

configuration. Generation schemes for atom-field entangled states [Eq. (1)] have been theoretically studied and experimentally implemented [38,43–45]. In the case of a scheme based on the off-resonant interaction [38], the required interaction Hamiltonian is

$$\hat{H}_I = \hbar \chi [(\hat{a}^\dagger \hat{a} + 1)|e\rangle\langle e| - \hat{a}^\dagger \hat{a}|g\rangle\langle g|], \tag{16}$$

and $\chi = \Omega^2/(4\delta)$ is the coupling constant determined by the vacuum Rabi frequency Ω and detuning δ [38]. As shown in Fig. 4, $\pi/2$ Ramsey pulse with phase $-\pi/2$ (R_A) is applied to a circular Rydberg atom (A) prepared in the excited state $|e\rangle_A$ [46], which results in an atomic superposition state: $|\phi_{-i}\rangle_A = (|e\rangle_A - i|g\rangle_A)/\sqrt{2}$. A strong dispersive interaction in Eq. (16) between atom A and the cavity field then produces the atom-field entangled state (1) for interaction time $t = \pi/(2\chi)$ [38].

Direct measurements of the light field in the microwave cavity are difficult to achieve, while indirect methods for parity measurements of the cavity field may be more feasible [12,24,38,47]. A circular Rydberg atom (B) in Fig. 4 initially prepared in state
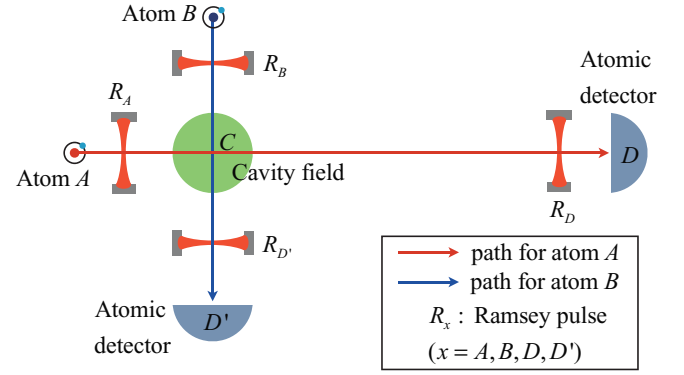
$|e\rangle_B$ evolves to a superposition state $|\phi_{-i}\rangle_B$ by $\pi/2$ Ramsey pulse with phase $-\pi/2$ (R_B), and the total state is $|\Psi_{\text{tot}}\rangle_{ABC} = |\Psi\rangle_{AC}|\phi_{-i}\rangle_B$. The displacement operation, $\hat{\mathcal{D}}_C^\dagger(\beta) = \hat{\mathcal{D}}_C(-\beta)$, is then applied to the field right before atom B enters the cavity, and the same type of interaction as Eq. (16) between modes B and C follows. One may indirectly detect the cavity field by appropriately choosing the interaction time $t = \pi/(2\chi)$ between atom B and the field before detecting the atom. The interaction time may be controlled by selecting the velocity of atom B. The final measurement for atom A, represented by $\hat{\Gamma}_A(-\pi e^{-i\phi}/4)$, is performed using $\pi/2$ Ramsey pulse of phase $\pi - \phi$ (R_D) and atomic detector D. The measurement on atom B, i.e., $\hat{\Gamma}_B(-\pi/4)$, for indirect probing is performed with the help of $\pi/2$ Ramsey pulse with π phase ($R_{D'}$) and atomic detector D'. The measurement operator is then represented as

$$\hat{\Upsilon}_{B,C}(\beta,t) = \hat{\mathcal{U}}_{B,C}(\beta,t)^\dagger \hat{\mathcal{O}}_{B,C} \hat{\mathcal{U}}_{B,C}(\beta,t), \tag{17}$$

where

$$\hat{\mathcal{O}}_{B,C} = [|+\rangle\langle+| - |-\rangle\langle-|]_B \otimes \mathbb{1}_C,$$
$$\hat{\mathcal{U}}_{B,C} = e^{-i\hat{H}_I t/\hbar}_{B,C} \hat{\mathcal{D}}_C^\dagger(\beta),$$

and $|\pm\rangle = (|e\rangle \pm |g\rangle)/\sqrt{2}$. The correlation function $E(\zeta,\beta,t) = \langle\hat{\Gamma}_A(\zeta) \otimes \hat{\Upsilon}_{B,C}(\beta,t)\rangle$ is calculated using state $|\Psi_{\text{tot}}\rangle_{ABC}$ as

$$
\begin{aligned}
E(\zeta,\beta,t) = {} & \tfrac{1}{2}\cos\theta\, e^{(|\alpha|^2+|\beta|^2-2|\alpha||\beta|\cos\Phi)(-1+\cos 2\chi t)} \cos[(|\alpha|^2 + |\beta|^2 - 2|\alpha||\beta|\cos\Phi)\sin 2\chi t] \\
& - \tfrac{1}{2}\cos\theta\, e^{(|\alpha|^2+|\beta|^2+2|\alpha||\beta|\cos\Phi)(-1+\cos 2\chi t)} \cos[(|\alpha|^2 + |\beta|^2 + 2|\alpha||\beta|\cos\Phi)\sin 2\chi t] \\
& + \tfrac{1}{2}\sin\theta\, e^{-|\alpha|^2-|\beta|^2-(|\alpha|^2-|\beta|^2)\cos 2\chi t - 2|\alpha||\beta|\sin\Phi\sin 2\chi t} \cos[\phi - (|\alpha|^2 - |\beta|^2)\sin 2\chi t + 2|\alpha||\beta|\sin\Phi(-1 + \cos 2\chi t)] \\
& + \tfrac{1}{2}\sin\theta\, e^{-|\alpha|^2-|\beta|^2-(|\alpha|^2-|\beta|^2)\cos 2\chi t + 2|\alpha||\beta|\sin\Phi\sin 2\chi t} \cos[\phi + (|\alpha|^2 - |\beta|^2)\sin 2\chi t + 2|\alpha||\beta|\sin\Phi(-1 + \cos 2\chi t)]
\end{aligned}
\tag{18}
$$

and the Bell function, $\mathcal{B}_\Upsilon$, is accordingly obtained. As expected, the optimizing conditions for $|\mathcal{B}_\Upsilon|_{\max}$ are identical to those for $|\mathcal{B}_\mathcal{O}|_{\max}$ in Eqs. (14) and (15) with an additional

condition, $t = t' = \pi/2\chi$. Our numerical study confirms that the optimized Bell function $|\mathcal{B}_\Upsilon|_{\max}$ plotted with the above-mentioned conditions in Fig. 5 exactly overlaps with the solid
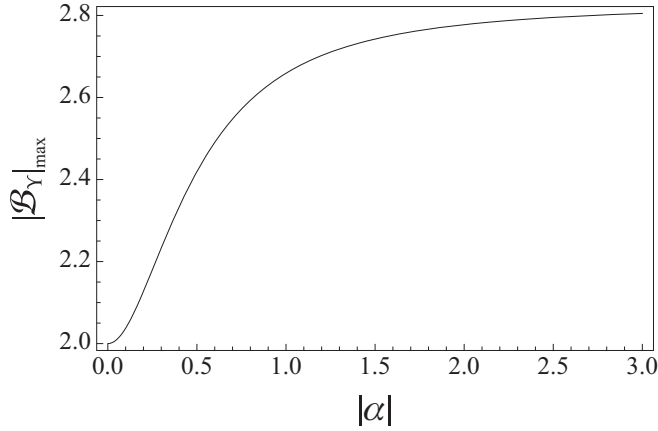
FIG. 5. Numerically optimized values of Bell function $\mathcal{B}_\Upsilon$ with indirect measurements against $|\alpha|$. The result is found to be identical to the one using direct parity measurements shown as the solid curve in Fig. 3.

curve in Fig. 3 as shown. This result is due to the fact that the indirect measurement (17) is basically equivalent to the displaced parity measurement (12) on the cavity field when t is chosen to be $\pi/(2\chi)$ [47], i.e., the measurement on atom B in the basis $\{|+\rangle, |-\rangle\}$ after the interaction time $t = \pi/(2\chi)$ is equivalent to the parity measurement on the cavity field. In fact, it can be shown that the correlation functions (18) with $t = \pi/(2\chi)$ and (13) are identical. Of course, if we restrict ζ to be real, the optimized plot of the Bell function $|\mathcal{B}_\Upsilon|_{\max}$ approaches the dashed curve in Fig. 3.

V. DECOHERENCE AND LOOPHOLES

It is not difficult to predict that decoherence effects due to the cavity-field dissipation and the spontaneous emission of the atoms will obstruct Bell violations. This is particularly important when one intends to demonstrate a Bell violation free from the loopholes. In this section, we consider decoherence effects with realistic conditions for the Bell-CHSH inequality test using parity measurements and suggest quantitative requirements to perform a loophole-free Bell test.

A. Decoherence effects in the cavity-atom system

There are two main effects that cause decoherence in our Bell inequality test, i.e., spontaneous emissions from atoms and cavity field dissipations. In the atom-cavity system under consideration, one (or both) of these two effects may occur. The master equation which determines the time evolution of the density operator, $\hat{\rho}(t)$, under the atom-field interaction with spontaneous emissions and cavity dissipations is

$$\frac{d\hat{\rho}(t)}{dt} = \frac{1}{i\hbar}[\hat{H}_I, \hat{\rho}(t)] + \mathcal{L}\hat{\rho}(t), \tag{19}$$

with the Linblad decohering term $\mathcal{L}$ defined as

$$\mathcal{L}\hat{\rho} \equiv \kappa(2\hat{a}\hat{\rho}\hat{a}^\dagger - \hat{a}^\dagger\hat{a}\hat{\rho} - \hat{\rho}\hat{a}^\dagger\hat{a})$$
$$+ \gamma(2\hat{\sigma}_-\hat{\rho}\hat{\sigma}_+ - \hat{\sigma}_+\hat{\sigma}_-\hat{\rho} - \hat{\rho}\hat{\sigma}_+\hat{\sigma}_-), \tag{20}$$
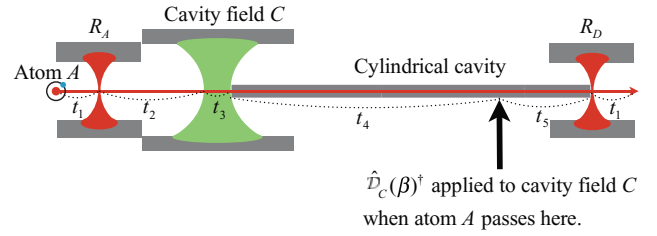

FIG. 6. (Color online) Sideview of the atom A's path with intervals of time. Each interval denotes an amount of time required for atom A to pass through the region related with atomic velocity v. We note that the distance $l = v \times (t_4 + t_5)$, which corresponds to the length of the cylindrical cavity, is a crucial factor in a loohole-free Bell inequality test.

where κ is the dissipation rate of cavity field and γ is the spontaneous emission rate.

It is known that the spontaneous emission rate of an atom can be significantly reduced by engineering the shape of the cavity that contains the atom [48,49]. A complete inhibition of spontaneous emission was suggested using a cylindrical metal cavity with a diameter shorter than $1.8412c/\omega_0$, where ω_0 is the transition rate between atomic states $|e\rangle$ and $|g\rangle$ and c is the speed of light [49]. For our setup, the transition rate can be taken from Ref. [24] as $\omega_0 = 51.1$ GHz. This means that the diameter should be smaller than 3.44 mm, that is, experimentally achievable. As seen in Fig. 6, a long cylindrical cavity may be used between cavity C and Ramsey zone R_D to inhibit spontaneous emission.

The spontaneous emission rate γ_c inside the cavity C in Fig. 4 also generally differs from the spontaneous emission rate γ_0 in the vacuum. It is known that γ_c can be calculated by approximating the cavity in the one dimension while considering the effect of the atomic motion as described in Ref. [50]. In our case, $\gamma_c = 4.08$ Hz is obtained based on the result of Ref. [50] from the spontaneous emission rate in the vacuum, $\gamma_0 = 1/(2T_0)$ ($T_0 = 36$ ms is the atomic life time in the vacuum [38]) and related realistic parameters in a recent experiment [24].

Considering the discussions above, we present a timeline of decoherence effects in Fig. 7 together with time intervals required to pass through certain parts of the apparatus as follows (also depicted in Fig. 6): t_1 is a half of the time required for an atom to pass through a cavity used for Ramsey pulse application, t_2 is a half of the time required for an atom to pass through Ramsey pulse and the main cavity (C) without cavity waist, t_3 for an atom to pass through the main cavity(C)'s waist $(\pi/2\chi)$, t_4 for atom A to pass through the long cylindrical cavity before the field displacement operation on the cavity field, t_5 for atom A to pass through the remainder of the long cavity after the field displacement operation, and t_6 for atomic detection at D or D'.

Let us, first, consider the pathway of atom A, which corresponds to the top line of Fig. 7. Atom A undergoes spontaneous emission before and after the Ramsey pulse R_A with rate γ_0 (diagonally hatched part). Atom A then interacts with the cavity field with dissipation rate κ under spontaneous emission (γ_c), which is represented by the horizontally hatched part. After the atom-field interaction, atom A passes through
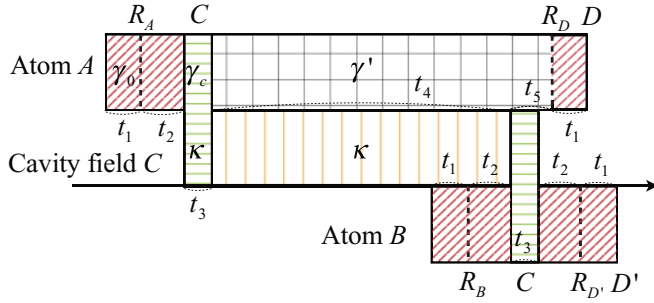
FIG. 7. (Color online) A timeline for decoherence with dynamical parameters related in each regions (from left to right). The top line is for atom A, the middle for cavity field C, and the bottom for atom B. The times when Ramsey pulses are applied are described as vertical dashed lines. We consider a Ramsey pulse application as an instant event as a Ramsey pulse lasts as short as 1 μs order [45]. Regions are differently hatched depending on the types of dynamics. In the diagonally hatched regions, atoms A and B travel in free spaces with the spontaneous emission rate γ_0 before and after Ramsey pulses as shown in Fig. 4. In the cross-hatched region, atom A travels in a cylindrical cavity with the inhibited spontaneous emission rate γ'. In the vertically hatched region, the cavity dissipation with rate κ occurs in the cavity (C) field. The horizontally hatched regions correspond to the dynamics of the atom-field interaction $\hat{H}_I$ in the main cavity C together with spontaneous emission γ_c and cavity dissipation κ. Abbreviations C, D, D', R_A, R_B, R_D, and $R_{D'}$ are consistent with those in Fig. 4.

the cylindrical cavity experiencing inhibited spontaneous emission (γ'). Finally, atom A comes out of Ramsey pulse R_D experiencing spontaneous emission (γ_0) and is registered at detector D. In the meantime, cavity field C which has interacted with atom A undergoes field dissipation (κ) while atom A is passing through cylindrical cavity. Cavity field C then begins to interacts with atom B under spontaneous emission (γ_c) and field dissipation (κ) after displacement operation on it. Atom B, used for an indirect measurement, experiences spontaneous emission (γ_0) around Ramsey pulse R_B, interaction with the cavity field (C) with spontaneous emission (γ_c), and spontaneous emission (γ_0) before detection D'.

Here, we take the photon storage time $T_C = 0.13$s ($\kappa = 1/(2T_C)$), $\Omega = 2\pi \times 49$ kHz and $\delta = 2\pi \times 65$ kHz ($\chi = \Omega^2/(4\delta) \approx 58$ kHz) from recent experiments [24]. The solution of the master equation for the cavity dissipation alone with H_I was examined in Ref. [51]. In the appendix, we obtain the solution of Eq. (19) and find an explicit form of the density operator and the correlation function. The Bell function can be constructed using the correlation function in Eq. (B13) of the appendix. Note that we have assumed perfect Ramsey pulses during the procedures. Considering cavity dissipation, we employ the same optimizing conditions (14) except that $|\beta|$ is chosen to be the values that satisfy

$$\frac{|\alpha|e^{-\kappa(t_4+t_3)} - |\beta|}{|\alpha|e^{-\kappa(t_4+t_3)} + |\beta|} = \tan(4|\alpha|e^{-\kappa(t_4+t_3)}|\beta|) \qquad (21)$$
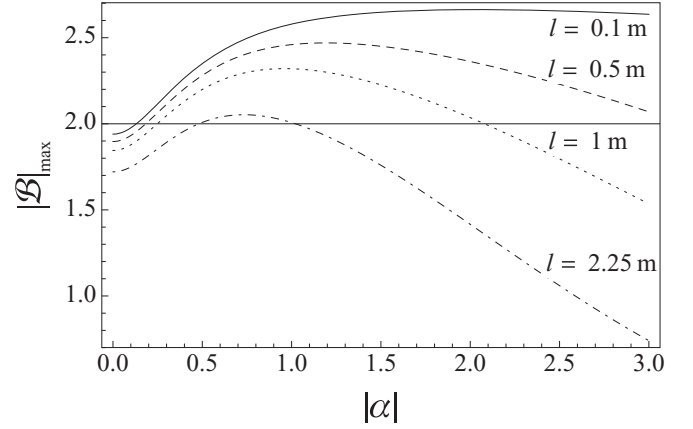
and is nearest to zero.

FIG. 8. The Bell function under realistic conditions discussed in Sec. V B are plotted with optimizing conditions in Eqs. (14) and (21) for several different cases of separation l. As the separation l increases, the maximum values of the Bell function decrease. The decoherence effects become heavier as $|\alpha|$ increases.

B. Bell violation and separations under practical conditions without a cylindrical cavity

Let us, first, consider Bell violation depending on the separation $l = v \times (t_4 + t_5)$ between both parties *without* using a cylindrical cavity (thus, $\gamma' = \gamma_0$). We choose some practical time-interval parameters as $t_1 = 80.0$ μs, $t_2 = 166.5$ μs, $t_3 = 27.1$ μs, $t_6 = 20$ μs and velocity of an atom $v = 250$ m/s [24,52]. The Bell function with several choices of l are plotted in Fig. 8. The Bell function approaches the value near 2.7 when $l = 0.1$ (meter), but it decreases as l gets larger. Clear Bell violations appear for $l \lesssim 2$ (meter), however, this is insufficient for a spacelike separation as we shall discuss in the next subsection.

C. Requirements for a Bell test free from the locality loophole with a cylindrical cavity

In principle, a Bell test free from the locality loophole can be performed using a long cylindrical cavity with a low spontaneous emission rate (γ') and the main cavity with a low dissipation rate (κ). In order to close the locality loophole, the measurement event for atom A should not affect the measurement event for the cavity field C, and *vice versa* [11]. In other words, the measurement event for atom A should be outside of the "back light cone" from the detection event D' in Fig. 4. In the same manner, the measurement event for the cavity field C should not be in the back light cone from the detection event D. For simplicity, let us first suppose that each measurement process takes place at a single location (D and D'). In our Bell test, the time t_A required to measure atom A is smaller than the time required to measure field C (t_C) due to the indirect measurement scheme for field C. We assume that the measurement event for the field C precedes to the measurement event for atom A by T (the opposite case will require a longer separation between the two parties). The conditions required to close the locality loophole then are

$$d \geqslant c(T + t_A),$$
$$d \geqslant c(t_C - T), \qquad (22)$$

where d is the distance between D and D' and c is the speed of light.

In order to apply the locality-loophole-free conditions (22) to our Bell test setup in a more rigorous manner, one needs to consider locations of the local measurement elements. In Fig. 7, one can find that the measurement time for atom A (t_A) consists of the times for R_D (t_1) and D (t_6) and that for the field (t_C) consists of the times for C (t_3), R'_D ($t_2 + t_1$), and D' (t_6). A measurement event for each party actually does not take place at a single location, and both of the measurements are not even on a straight line. Therefore the distance d in Eqs. (22) needs to be replaced with the distances from the final detector of one party to the location where the measurement of the other party begins. A careful consideration leads to the conclusion that the following inequalities should be satisfied:

$$v(t_3/2 + t_4 + t_5 + t_1 + t_6) \geqslant c(t_5 + t_1 + t_6),$$
$$v\sqrt{(t_3/2 + t_2 + t_1 + t_6)^2 + (t_3/2 + t_4 + t_5)^2} \qquad (23)$$
$$\geqslant c(t_3 + t_2 + t_1 + t_6 - t_5).$$

Using the feasible values of t_1, t_2, t_3, t_6 and v in the previous subsection, we find the minimum values $t_4 = 236.0$ s and $t_5 = 96.8$ μs with which the equalities hold for Eqs. (23). The minimum distance required for a Bell test free from the locality loophole then is found to be $l = 52.99$ km [24].

We, finally, consider conditions of the atomic life time $T_{atom} = 1/(2\gamma')$ and the photon storage time $T_c = 1/(2\kappa)$ required for a Bell test free from the locality loophole. In Fig. 9, we plot the Bell function constructed using Eq. (B13) in the appendix with respect to the photon storage time in the main cavity and amplitude $|\alpha|$ of the atom-field entanglement. Here,
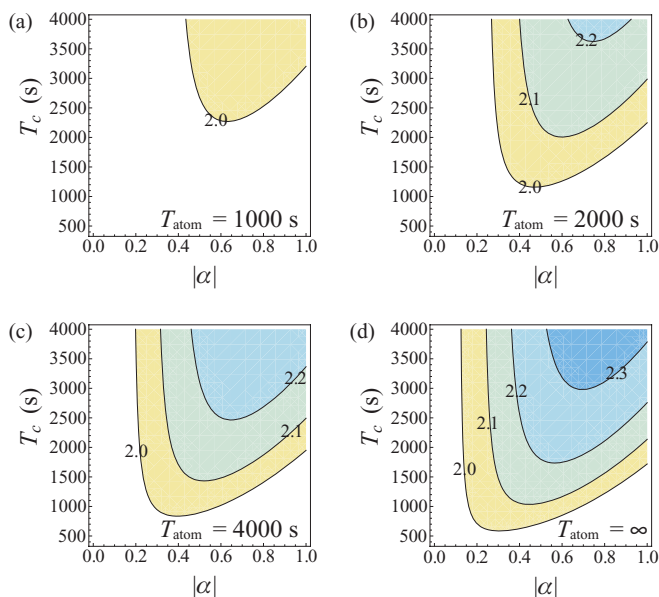

FIG. 9. (Color online) Contour plots of the Bell function with respect to photon storage time T_C in the main cavity and amplitude $|\alpha|$ of the entangled state. The atomic life time in cylindrical cavity T_{atom} is fixed at 1000, 2000, 4000, and ∞ (seconds). The minimum distance condition $l = 52.99$ (km) for a loophole-free Bell test was assumed. Higher inhibition of spontaneous emission in the cylindrical cavity reduces the required photon storage time in the main cavity.

the extended lifetime of the atom in the cylindrical cavity was assumed to be $T_{atom} = 1000, 2000, 4000,$ and ∞ (seconds). The distance l was assumed to be the minimum distance required for a loophole-free Bell test (52.99 km). For example, when $T_{atom} = 2000$ (seconds), the photon storage time $T_C \sim 1160$ (seconds) at $|\alpha| \sim 0.47$ is required to see a Bell violation. If complete inhibition of the spontaneous emission in the cylindrical cavity is possible, (i.e., $T_{atom} = \infty$), $T_C \sim 590$ at $|\alpha| \sim 0.3$ is required. Obviously, the stronger inhibition of the spontaneous emission in the cylindrical cavity relaxes the requirement of the photon storage time in the main cavity to see Bell violations. However, it still requires at least a few hundreds of seconds for the photon storage time to demonstrate a loophole-free Bell violation, while it is only about 0.13 s at present [53]. It would also be extremely challenging to build a long cylindrical cavity that strongly inhibits the spontaneous emission of atom A during such a long lifetime.

VI. REMARKS

We have investigated Bell-CHSH inequality tests with entanglement between a two-level atom and a coherent-state field in a cavity. In order to detect the cavity field for these tests, photon on-off measurements and photon number parity measurements, respectively, have been attempted. When photon on-off measurements with the perfect efficiency are used, the maximum value of the Bell violation is $|\mathcal{B}_\mathcal{O}| \approx 2.61$ at $|\alpha| \approx 0.664$. In order to see a violation of the Bell-CHSH inequality, at least 50% of detection efficiency is required. When photon parity measurements are used, the value of the Bell-CHSH violation rapidly increases as α gets larger, and it approaches Cirel'son's bound for $\alpha \gg 1$. Although precise direct measurements of cavity fields are experimentally difficult, photon number parity measurements for the cavity field can be effectively performed using ancillary probe atoms and atomic detectors. We have fully analyzed decoherence effects in both field and atomic modes and discuss conditions required to perform a Bell inequality test free from the locality loophole.

Our proposal may be considered an attempt to analyze a Bell inequality test using entanglement between a microscopic system and a mesoscopic classical system. Since atomic detectors are known to be highly efficient [54], it may also be a reasonable target to perform this type of experiment in a way free from the detection loophole. In principle, a Bell inequality test free from the locality loophole in our framework using atom-field entanglement may be performed using a long cylindrical cavity for the atom with a low spontaneous emission rate [49]. However, our analysis shows that it would be extremely demanding to perform a Bell inequality test free from both the locality and detection loopholes in this framework since the main cavity for field with a low dissipation rate would be necessary together with a long cylindrical cavity.

APPENDIX A: SOLUTIONS OF THE MASTER EQUATION FOR MATRIX ELEMENTS

We first find general solutions of the master equation [Eq. (19)] for three types of decoherence processes step by step, i.e., spontaneous emission of an atom, cavity dissipation, and atom-field interaction with spontaneous emission and cavity dissipation.

1. Spontaneous emission for atom

A density operator of a two-level atom, $\hat{\rho}_A(t)$, can be expressed as a matrix form,

$$\hat{\rho}_A(t) = \begin{pmatrix} \rho_{A,ee}(t) & \rho_{A,eg}(t) \\ \rho_{A,ge}(t) & \rho_{A,gg}(t) \end{pmatrix}, \qquad (A1)$$

where $\rho_{A,ij}(t) = \langle i|\hat{\rho}_A(t)|j\rangle$. When an atom with a initial density matrix, $\hat{\rho}_A(0)$, goes through the spontaneous emission process for time t, its density matrix is straightforwardly obtained using Eq. (19) with $\chi = 0$ and $\kappa = 0$ as

$$\begin{aligned} \hat{\rho}_A(t) &= \hat{\mathcal{S}}_A(\gamma,t)[\hat{\rho}_A(0)] \\ &= \begin{pmatrix} e^{-2\gamma t}\rho_{A,ee}(0) & e^{-\gamma t}\rho_{A,eg}(0) \\ e^{-\gamma t}\rho_{A,ge}(0) & \rho_{A,gg}(0) - \rho_{A,ee}(0)(e^{-2\gamma t}-1) \end{pmatrix}, \end{aligned}$$
$$(A2)$$

where superoperator $\hat{\mathcal{S}}(\gamma,t)$ is defined for later use.

2. Dissipation for cavity field

In order to find the time evolution of the coherent-state part the density operator, it is sufficient to find the time evolution of an operator component $|\mu\rangle\langle\nu|$, where $|\mu\rangle$ and $|\nu\rangle$ are coherent states of amplitudes μ and ν. This solution for time t under the master equation [Eq. (19)] with $\chi = 0$ and $\gamma = 0$ is well known as [55,56]

$$\begin{aligned} &\exp\left[-\frac{(|\mu|^2 + |\nu|^2 - 2\nu^*\mu)(1 - \exp(-2\kappa t))}{2}\right] \\ &\times |\mu e^{-\kappa t}\rangle\langle\nu e^{-\kappa t}|. \end{aligned} \qquad (A3)$$

3. Atom-field interaction with spontaneous emission and cavity dissipation

The density matrix $\hat{\rho}(t)$ for an atom-field state can be considered in a $(2 \times \infty)$-dimensional space, since we assume a two-level atom. It is possible to decompose the master equation [Eq. (19)] in $\{|e\rangle, |g\rangle\}$ basis with the density matrix elements $\hat{\rho}_{C,ij}(t) = \langle i|\hat{\rho}(t)|j\rangle$. We then obtain equations

$$\begin{aligned} \frac{d}{dt}\hat{\rho}_{C,ee} &= \hat{\mathcal{L}}_{ee}\hat{\rho}_{C,ee} - 2\gamma\hat{\rho}_{C,ee} \\ &= -i\chi[\hat{a}^\dagger\hat{a},\hat{\rho}_{C,ee}] + \kappa(2\hat{a}\hat{\rho}_{C,ee}\hat{a}^\dagger - \hat{a}^\dagger\hat{a}\hat{\rho}_{C,ee} \\ &\quad - \hat{\rho}_{C,ee}\hat{a}^\dagger\hat{a}) - 2\gamma\hat{\rho}_{C,ee}, \end{aligned} \qquad (A4)$$

$$\begin{aligned} \frac{d}{dt}\hat{\rho}_{C,gg} &= \hat{\mathcal{L}}_{gg}\hat{\rho}_{C,gg} + 2\gamma\hat{\rho}_{C,ee} \\ &= i\chi[\hat{a}^\dagger\hat{a},\hat{\rho}_{C,gg}] + \kappa(2\hat{a}\hat{\rho}_{C,gg}\hat{a}^\dagger - \hat{a}^\dagger\hat{a}\hat{\rho}_{C,gg} \\ &\quad - \hat{\rho}_{C,gg}\hat{a}^\dagger\hat{a}) + 2\gamma\hat{\rho}_{C,ee}, \end{aligned} \qquad (A5)$$

$$\begin{aligned} \frac{d}{dt}\hat{\rho}_{C,eg} &= \hat{\mathcal{L}}_{eg}\hat{\rho}_{C,eg} - i\chi\hat{\rho}_{C,eg} - \gamma\hat{\rho}_{C,eg} \\ &= -i\chi(\hat{a}^\dagger\hat{a} + 1)\hat{\rho}_{C,eg} - i\chi\hat{\rho}_{C,eg}\hat{a}^\dagger\hat{a} \\ &\quad + \kappa(2\hat{a}\hat{\rho}_{C,eg}\hat{a}^\dagger - \hat{a}^\dagger\hat{a}\hat{\rho}_{C,eg} - \hat{\rho}_{C,eg}\hat{a}^\dagger\hat{a}) - \gamma\hat{\rho}_{C,eg}, \end{aligned} \qquad (A6)$$

$$\begin{aligned} \frac{d}{dt}\hat{\rho}_{C,ge} &= \hat{\mathcal{L}}_{ge}\hat{\rho}_{C,ge} + i\chi\hat{\rho}_{C,ge} - \gamma\hat{\rho}_{C,ge} \\ &= i\chi\hat{\rho}_{C,ge}(\hat{a}^\dagger\hat{a} + 1) + i\chi\hat{a}^\dagger\hat{a}\hat{\rho}_{C,ge} \\ &\quad + \kappa(2\hat{a}\hat{\rho}_{C,ge}\hat{a}^\dagger - \hat{a}^\dagger\hat{a}\hat{\rho}_{C,ge} - \hat{\rho}_{C,ge}\hat{a}^\dagger\hat{a}) - \gamma\hat{\rho}_{C,ge}. \end{aligned} \qquad (A7)$$

We define the following superoperators for simplicity: $\hat{\mathcal{M}} = \hat{a}^\dagger\hat{a}\cdot$, $\hat{\mathcal{P}} = \cdot\hat{a}^\dagger\hat{a}$, and $\hat{\mathcal{J}} = \hat{a}\cdot\hat{a}^\dagger$. Then $\hat{\mathcal{L}}_{ee}$, $\hat{\mathcal{L}}_{gg}$, $\hat{\mathcal{L}}_{eg}$, and $\hat{\mathcal{L}}_{ge}$ can be expressed as

$$\hat{\mathcal{L}}_{ee} \equiv 2\kappa\hat{\mathcal{J}} - r\hat{\mathcal{M}} - r^*\hat{\mathcal{P}}, \qquad (A8a)$$
$$\hat{\mathcal{L}}_{eg} \equiv 2\kappa\hat{\mathcal{J}} - r\hat{\mathcal{M}} - r\hat{\mathcal{P}}, \qquad (A8b)$$

where $r \equiv \kappa + i\chi$ and $\hat{\mathcal{L}}_{gg}$ and $\hat{\mathcal{L}}_{ge}$ are obtained by substituting χ with $-\chi$ in $\hat{\mathcal{L}}_{ee}$, and $\hat{\mathcal{L}}_{eg}$, respectively. A master equation of the form $d\hat{\rho}/dt = \hat{\mathcal{L}}\hat{\rho} + c\hat{\rho}$, where c is a constant and $\hat{\mathcal{L}}$ is a superoperator, can be solved with a usual exponential form $\exp[(\hat{\mathcal{L}} + c)t]\hat{\rho}$.

a. Solution for $\hat{\rho}_{C,ee}$

The solution of Eq. (A4) is

$$\hat{\rho}_{C,ee}(t) = \exp[(\hat{\mathcal{L}}_{ee} - 2\gamma)t]\hat{\rho}_{C,ee}(0) = e^{-2\gamma t}e^{\hat{\mathcal{L}}_{ee}t}\hat{\rho}_{C,ee}(0), \qquad (A9)$$

where the factorization can be done by the similarity transformation [57]. Now we need to factorize $e^{\hat{\mathcal{L}}_{ee}t}$. This is solved with an ansatz (a technique can be found in Ref. [56])

$$\begin{aligned} \hat{\rho}_{C,ee}(t) &= \exp[-2\gamma t]\exp[(-r\hat{\mathcal{M}} - r^*\hat{\mathcal{P}})t] \\ &\quad \times \exp[f(t)2\kappa\hat{\mathcal{J}}]\hat{\rho}_{C,ee}(0), \end{aligned} \qquad (A10)$$

where $f(t) = (1 - e^{-2\kappa t})/(2\kappa)$. For an initial state $\hat{\rho}_{C,ee}(0) = |\mu\rangle\langle\nu|$,

$$\hat{\rho}_{C,ee}(t) = \exp[-2\gamma t + \Theta(\kappa,0,\mu,\nu,t)]|\mu e^{-rt}\rangle\langle\nu e^{-rt}| \quad (A11)$$

with

$$\begin{aligned} \Theta(\kappa,\chi,\mu,\nu,t) &:= -\frac{1}{2}(|\nu|^2 + |\mu|^2)(1 - e^{-2\kappa t}) \\ &\quad + \frac{\kappa}{r}(1 - e^{-2rt})\nu^*\mu. \end{aligned} \qquad (A12)$$

b. Solution for $\hat{\rho}_{C,gg}$

In order to solve Eq. (A5), we first assume $\gamma = 0$. A homogeneous solution is obtained from Eq. (A11) by

substituting χ with $-\chi$ as

$$\hat{\rho}_{C,gg}^h(t) = \exp[\Theta(\kappa,0,\mu,\nu,t)]|\mu e^{-r^*t}\rangle\langle\nu e^{-r^*t}|. \quad \text{(A13)}$$

It is then obvious to see that the general solution $\hat{\rho}_{C,gg}(t)$ with $\gamma \neq 0$ is

$$\hat{\rho}_{C,gg}(t) = \hat{\rho}_{C,gg}^h(t) + 2\gamma \int_0^t dt' \hat{\rho}_{C,ee}(t')$$

$$= \exp[\Theta(\kappa,0,\mu,\nu,t)]|\mu e^{-r^*t}\rangle\langle\nu e^{-r^*t}|$$

$$+ 2\gamma \int_0^t dt' \exp[-2\gamma t'$$

$$+ \Theta(\kappa,0,\mu,\nu,t')]|\mu e^{-rt'}\rangle\langle\nu e^{-rt'}|.$$

(A14)

c. Solution for $\hat{\rho}_{C,ge}$

The solution of Eq. (A7) is

$$\hat{\rho}_{C,ge}(t) = \exp[(\hat{\mathcal{L}}_{ge} + i\chi - \gamma)t]\hat{\rho}_{C,ge}(0)$$

$$= e^{(i\chi-\gamma)t}e^{\hat{\mathcal{L}}_{ge}t}\hat{\rho}_{C,ge}(0). \quad \text{(A15)}$$

Factoring $e^{\hat{\mathcal{L}}_{eg}t}$ with an ansatz

$$\hat{\rho}_{C,ge}(t) = \exp[(i\chi - \gamma)t]\exp[(-r\hat{\mathcal{M}} - r^*\hat{\mathcal{P}})t]$$

$$\times \exp[g(t)2\kappa\hat{\mathcal{J}}]\hat{\rho}_{C,ee}(0), \quad \text{(A16)}$$

where $g(t) = (1 - e^{-2r^*t})/(2r^*)$. For $\hat{\rho}_{C,ge}(0) = |\mu\rangle\langle\nu|$,

$$\hat{\rho}_{C,ge}(t) = \exp[(i\chi - \gamma)t + \Theta(\kappa,-\chi,\mu,\nu,t)]|\mu e^{-r^*t}\rangle\langle\nu e^{-rt}|. \quad \text{(A17)}$$

d. Solution for $\hat{\rho}_{C,eg}$

The solution of Eq. (A6) is obtained from Eq. (A17) by substituting χ with $-\chi$ as

$$\hat{\rho}_{C,eg}(t) = \exp[(-i\chi - \gamma)t + \Theta(\kappa,\chi,\mu,\nu,t)]|\mu e^{-rt}\rangle\langle\nu e^{-r^*t}|. \quad \text{(A18)}$$

APPENDIX B: DERIVATION OF THE DENSITY MATRICES FOR ATOM-FIELD ENTANGLEMENT AND THE CORRELATION FUNCTION

1. Atom-field entanglement generated under decoherence effects

First, atom A initially prepared in $|e\rangle_A$ undergoes the spontaneous emission for the time t_1. After applying the first Ramsey pulse, $R_A = \hat{D}_A(-i\pi/4)$, explained in Sec. IV, atom A again undergoes the spontaneous emission for time t_2. Using Eqs. (A2) again, it becomes

$$\hat{\mathcal{S}}_A(\gamma_0,t_2)[\hat{D}_A(-i\pi/4)|\{\hat{\mathcal{S}}_A(\gamma_0,t_1)[(|e\rangle\langle e|)_A]\}\hat{D}_A^\dagger(-i\pi/4)]$$

$$= \begin{pmatrix} \frac{1}{2}e^{-2\gamma_0 t_2} & \left(-\frac{i}{2} + ie^{-2\gamma_0 t_1}\right)e^{-\gamma_0 t_2} \\ \left(\frac{i}{2} - ie^{-2\gamma_0 t_1}\right)e^{-\gamma_0 t_2} & \left(1 - \frac{1}{2}e^{-2\gamma_0 t_2}\right) \end{pmatrix}. \quad \text{(B1)}$$

Then atom A interacts with the cavity field C prepared in state $|i\alpha\rangle_C$. Using Eqs. (A11), (A14), (A17), and (A18), we find the state after the interaction time t_3 as $\hat{\rho}_{AC}^{(3)}$ with its matrix elements:

$$\hat{\rho}_{AC,ee}^{(3)} = \frac{1}{2}e^{-2\gamma_0 t_2 - 2\gamma_c t_3}|i\alpha e^{-rt_3}\rangle\langle i\alpha e^{-rt_3}|, \quad \text{(B2a)}$$

$$\hat{\rho}_{AC,eg}^{(3)} = \left(-\frac{i}{2} + ie^{-2\gamma_0 t_1}\right)\exp[-\gamma_0 t_2 + (-i\chi - \gamma_c)t_3$$

$$+ \Theta(\kappa,\chi,\alpha,\alpha,t_3)]|i\alpha e^{-rt_3}\rangle\langle i\alpha e^{-r^*t_3}|, \quad \text{(B2b)}$$

$$\hat{\rho}_{AC,ge}^{(3)} = \left(\frac{i}{2} - ie^{-2\gamma_0 t_1}\right)\exp[-\gamma_0 t_2 + (i\chi - \gamma_c)t_3$$

$$+ \Theta(\kappa,-\chi,\alpha,\alpha,t_3)]|i\alpha e^{-r^*t_3}\rangle\langle i\alpha e^{-rt_3}|, \quad \text{(B2c)}$$

$$\hat{\rho}_{AC,gg}^{(3)} = \left(1 - \frac{1}{2}e^{-2\gamma_0 t_2}\right)|i\alpha e^{-r^*t_3}\rangle\langle i\alpha e^{-r^*t_3}|$$

$$+ 2\gamma_c \int_0^{t_3} dt \frac{1}{2}e^{-2\gamma_0 t_2 - 2\gamma_c t}|i\alpha e^{-rt}\rangle\langle i\alpha e^{-rt}|. \quad \text{(B2d)}$$

2. Atom-field entanglement after traveling for the spacelike separation

We now derive the total density matrix right before $\hat{\mathcal{D}}_C^\dagger(\beta)$ is applied. The state $\hat{\rho}_{AC}^{(3)}$ undergoes spontaneous emission inside the cylindrical cavity and dissipation inside the cavity field C. The calculation can be done using the results in Sec. A3 with $\chi = 0$. The state then becomes $\hat{\rho}_{AC}^{(4)}$, where

$$\hat{\rho}_{AC,ee}^{(4)} = \frac{1}{2}e^{-2\gamma_0 t_2 - 2\gamma_c t_3 - 2\gamma' t_4}|i\alpha e^{-rt_3 - \kappa t_4}\rangle\langle i\alpha e^{-rt_3 - \kappa t_4}|, \quad \text{(B3a)}$$

$$\hat{\rho}_{AC,eg}^{(4)} = \left(-\frac{i}{2} + ie^{-2\gamma_0 t_1}\right)\exp[-\gamma_0 t_2 + (-i\chi - \gamma_c)t_3 - \gamma' t_4$$

$$+ \Theta(\kappa,\chi,\alpha,\alpha,t_3) + \Theta(\kappa,0,\alpha e^{-rt_3},\alpha e^{-r^*t_3},t_4)]$$

$$|i\alpha e^{-rt_3 - \kappa t_4}\rangle\langle i\alpha e^{-r^*t_3 - \kappa t_4}|, \quad \text{(B3b)}$$

$$\hat{\rho}_{AC,ge}^{(4)} = \left(\frac{i}{2} - ie^{-2\gamma_0 t_1}\right)\exp[-\gamma t_2 + (i\chi - \gamma_c)t_3 - \gamma' t_4$$

$$+ \Theta(\kappa,-\chi,\alpha,\alpha,t_3) + \Theta(\kappa,0,\alpha e^{-r^*t_3},\alpha e^{-rt_3},t_4)]$$

$$|i\alpha e^{-r^*t_3 - \kappa t_4}\rangle\langle i\alpha e^{-rt_3 - \kappa t_4}|, \quad \text{(B3c)}$$

$$\hat{\rho}_{AC,gg}^{(4)} = \left(1 - \frac{1}{2}e^{-2\gamma_0 t_2}\right)|i\alpha e^{-r^*t_3 - \kappa t_4}\rangle\langle i\alpha e^{-r^*t_3 - \kappa t_4}|$$

$$+ 2\gamma_c \int_0^{t_3} dt \frac{1}{2}e^{-2\gamma_0 t_2 - 2\gamma_c t}|i\alpha e^{-rt - \kappa t_4}\rangle\langle i\alpha e^{-rt - \kappa t_4}|$$

$$+ 2\gamma' \int_0^{t_4} dt \frac{1}{2}e^{-2\gamma_0 t_2 - 2\gamma_c t_3 - 2\gamma' t}|i\alpha e^{-rt_3 - \kappa t}\rangle$$

$$\times \langle i\alpha e^{-rt_3 - \kappa t}|, \quad \text{(B3d)}$$

and here the subscripts are consistent with the previous ones.

3. Effects with atom B for indirect measurement

After applying the displacement operation $\hat{\mathcal{D}}_C^\dagger(\beta)$, the total state becomes $\hat{\rho}_{AC}^\beta = \hat{\mathcal{D}}_C^\dagger(\beta)\hat{\rho}_{AC}^l\hat{\mathcal{D}}_C(\beta)$. Now, the probe atom B, which is in the same state as that of atom A in Eq. (B1), goes into the cavity field of state $\hat{\rho}_{AC}^\beta$. The atom-field interaction H_I with the coupling constant χ occurs between atom B and field C for time t_3. When solving the master equation, it is convenient if one notes that the field-part of state $\hat{\rho}_{AC}^\beta$ can be expressed by coherent-state dyadics such as $|\mu\rangle\langle\nu|$. If the component of the cavity field, initially prepared as $|\mu\rangle\langle\nu|$, interacts with an atomic state (B1) for time t_3, the resulting density operator element is obtained as

$\hat{\Omega}_{BC}(\mu,\nu,t_3)$ with

$$\hat{\Omega}_{BC,ee}(\mu,\nu,t_3) = \frac{1}{2}e^{-2\gamma_0 t_2 - 2\gamma_c t_3 + \Theta(\kappa,0,\mu,\nu,t_3)}|\mu e^{-rt_3}\rangle\langle\nu e^{-rt_3}|, \tag{B4a}$$

$$\hat{\Omega}_{BC,eg}(\mu,\nu,t_3) = \left(-\frac{i}{2} + ie^{-2\gamma_0 t_1}\right)\exp[-\gamma_0 t_2 + (-i\chi - \gamma_c)t_3 + \Theta(\kappa,\chi,\mu,\nu,t_3)]|\mu e^{-rt_3}\rangle\langle\nu e^{-r^*t_3}|, \tag{B4b}$$

$$\hat{\Omega}_{BC,ge}(\mu,\nu,t_3) = \left(\frac{i}{2} - ie^{-2\gamma_0 t_1}\right)\exp[-\gamma_0 t_2 + (i\chi - \gamma_c)t_3 + \Theta(\kappa,-\chi,\mu,\nu,t_3)]|\mu e^{-r^*t_3}\rangle\langle\nu e^{-rt_3}|, \tag{B4c}$$

$$\hat{\Omega}_{BC,gg}(\mu,\nu,t_3) = \left(1 - \frac{1}{2}e^{-2\gamma_0 t_2}\right)e^{\Theta(\kappa,0,\mu,\nu,t_3)}|\mu e^{-r^*t_3}\rangle\langle\nu e^{-r^*t_3}| + 2\gamma_c\int_0^{t_3}dt\frac{1}{2}e^{-2\gamma_0 t_2 - 2\gamma_c t + \Theta(\kappa,0,\mu,\nu,t)}|\mu e^{-rt}\rangle\langle\nu e^{-rt}|. \tag{B4d}$$

We used Eqs. (A11), (A14), (A17), and (A18) again to find Eqs. (B4a)–(B4d). Therefore, $\hat{\rho}_{AC}^\beta$ interacts with atom B and evolves to

$$\hat{\rho}_{ABC} = (|e\rangle\langle e|)_A \otimes \hat{\rho}_{BC,ee} + (|e\rangle\langle g|)_A \otimes \hat{\rho}_{BC,eg} + (|g\rangle\langle e|)_A \otimes \hat{\rho}_{BC,ge} + (|g\rangle\langle g|)_A \otimes \hat{\rho}_{BC,gg}, \tag{B5}$$

where

$$\hat{\rho}_{BC,ee} = \frac{1}{2}e^{-2\gamma_0 t_2 - 2\gamma_c t_3 - 2\gamma'(t_4 + t_3)}\hat{\Omega}_{BC}(i\alpha e^{-rt_3 - \kappa t_4} - \beta, i\alpha e^{-rt_3 - \kappa t_4} - \beta, t_3), \tag{B6a}$$

$$\hat{\rho}_{BC,eg} = \left(-\frac{i}{2} + ie^{-2\gamma_0 t_1}\right)\exp[-\gamma_0 t_2 + (-i\chi - \gamma_c)t_3 - \gamma'(t_4 + t_3) + \Theta(\kappa,\chi,\alpha,\alpha,t_3) + \Theta(\kappa,0,\alpha e^{-rt_3},\alpha e^{-r^*t_3},t_4)$$
$$- 2ie^{-\kappa(t_4 + t_3)}\sin(\chi t_3)\mathrm{Im}(\alpha^*\beta)]\hat{\Omega}_{BC}(i\alpha e^{-rt_3 - \kappa t_4} - \beta, i\alpha e^{-r^*t_3 - \kappa t_4} - \beta, t_3), \tag{B6b}$$

$$\hat{\rho}_{BC,ge} = \left(\frac{i}{2} - ie^{-2\gamma_0 t_1}\right)\exp[-\gamma_0 t_2 + (i\chi - \gamma_c)t_3 - \gamma'(t_4 + t_3) + \Theta(\kappa,-\chi,\alpha,\alpha,t_3) + \Theta(\kappa,0,\alpha e^{-r^*t_3},\alpha e^{-rt_3},t_4)$$
$$+ 2ie^{-\kappa(t_4 + t_3)}\sin(\chi t_3)\mathrm{Im}(\alpha^*\beta)]\hat{\Omega}_{BC}(i\alpha e^{-r^*t_3 - \kappa t_4} - \beta, i\alpha e^{-rt_3 - \kappa t_4} - \beta, t_3), \tag{B6c}$$

$$\hat{\rho}_{BC,gg} = \left(1 - \frac{1}{2}e^{-2\gamma_0 t_2}\right)\hat{\Omega}_{BC}(i\alpha e^{-r^*t_3 - \kappa t_4} - \beta, i\alpha e^{-r^*t_3 - \kappa t_4} - \beta, t_3)$$
$$+ 2\gamma_c\int_0^{t_3}dt\frac{1}{2}e^{-2\gamma_0 t_2 - 2\gamma_c t}\hat{\Omega}_{BC}(i\alpha e^{-rt - \kappa t_4} - \beta, i\alpha e^{-rt - \kappa t_4} - \beta, t_3) + 2\gamma'\int_0^{t_4}dt\frac{1}{2}e^{-2\gamma_0 t_2 - 2\gamma_c t_3 - 2\gamma' t}\hat{\Omega}_{BC}$$
$$\times (i\alpha e^{-rt_3 - \kappa t} - \beta, i\alpha e^{-rt_3 - \kappa t} - \beta, t_3) + \frac{1}{2}e^{-2\gamma_0 t_2 - 2\gamma_c t_3 - 2\gamma' t_4}\hat{\Omega}_{BC}(i\alpha e^{-rt_3 - \kappa t_4} - \beta, i\alpha e^{-rt_3 - \kappa t_4} - \beta, t_3)(1 - e^{-2\gamma' t_3}). \tag{B6d}$$

Spontaneous emissions of atom A and B that may occur after this point shall be taken into account when we derive the correlation function. Since the field state is not considered any more from this point before the final measurements, the cavity dissipation can be ignored. By tracing out the cavity field, we get

$$\hat{\rho}_{AB} = \mathrm{Tr}_C \hat{\rho}_{ABC} = \sum_{i,j=e,g}(|i\rangle\langle j|)_A \otimes \hat{\sigma}_{B,ij}, \tag{B7}$$

where

$$\hat{\sigma}_{B,ee} = \mathrm{Tr}_C \hat{\rho}_{BC,ee} = \frac{1}{2}e^{-2\gamma_0 t_2 - 2\gamma_c t_3 - 2\gamma'(t_4 + t_3)}\hat{U}_B(i\alpha e^{-rt_3 - \kappa t_4} - \beta, i\alpha e^{-rt_3 - \kappa t_4} - \beta, t_3), \tag{B8a}$$

$$\hat{\sigma}_{B,eg} = \left(-\frac{i}{2} + ie^{-2\gamma_0 t_1}\right)\exp[-\gamma_0 t_2 + (-i\chi - \gamma_c)t_3 - \gamma'(t_4 + t_3) + \Theta(\kappa,\chi,\alpha,\alpha,t_3) + \Theta(\kappa,0,\alpha e^{-rt_3},\alpha e^{-r^*t_3},t_4)$$
$$- 2ie^{-\kappa(t_4 + t_3)}\sin(\chi t_3)\mathrm{Im}(\alpha^*\beta)]\hat{U}_B(i\alpha e^{-rt_3 - \kappa t_4} - \beta, i\alpha e^{-r^*t_3 - \kappa t_4} - \beta, t_3), \tag{B8b}$$

$$\hat{\sigma}_{B,ge} = \left(\frac{i}{2} - ie^{-2\gamma_0 t_1}\right)\exp[-\gamma_0 t_2 + (i\chi - \gamma_c)t_3 - \gamma'(t_4 + t_3) + \Theta(\kappa,-\chi,\alpha,\alpha,t_3) + \Theta(\kappa,0,\alpha e^{-r^*t_3},\alpha e^{-rt_3},t_4)$$
$$+ 2ie^{-\kappa(t_4 + t_3)}\sin(\chi t_3)\mathrm{Im}(\alpha^*\beta)]\hat{U}_B(i\alpha e^{-r^*t_3 - \kappa t_4} - \beta, i\alpha e^{-rt_3 - \kappa t_4} - \beta, t_3), \tag{B8c}$$

$$\hat{\sigma}_{B,gg} = \left(1 - \frac{1}{2}e^{-2\gamma_0 t_2}\right)\hat{U}_B(i\alpha e^{-r^*t_3 - \kappa t_4} - \beta, i\alpha e^{-r^*t_3 - \kappa t_4} - \beta, t_3) + 2\gamma_c\int_0^{t_3}dt\frac{1}{2}e^{-2\gamma_0 t_2 - 2\gamma_c t}\hat{U}_B(i\alpha e^{-rt - \kappa t_4} - \beta, i\alpha e^{-rt - \kappa t_4} - \beta, t_3)$$
$$+ 2\gamma'\int_0^{t_4}dt\frac{1}{2}e^{-2\gamma_0 t_2 - 2\gamma_c t_3 - 2\gamma' t}\hat{U}_B(i\alpha e^{-rt_3 - \kappa t} - \beta, i\alpha e^{-rt_3 - \kappa t} - \beta, t_3)$$
$$+ \frac{1}{2}e^{-2\gamma_0 t_2 - 2\gamma_c t_3 - 2\gamma' t_4}\hat{U}_B(i\alpha e^{-rt_3 - \kappa t_4} - \beta, i\alpha e^{-rt_3 - \kappa t_4} - \beta, t_3)(1 - e^{-2\gamma' t_3}), \tag{B8d}$$

and operator $\hat{\mho}_B(\mu,\nu,t_3) = \text{Tr}_C \hat{\Omega}_{BC}(\mu,\nu,t_3)$ is determined as

$$\mho_{B,ee}(\mu,\nu,t_3) = \frac{1}{2} e^{-2\gamma_0 t_2 - 2\gamma_c t_3 + \Theta(\kappa,0,\mu,\nu,t_3) - \frac{1}{2}(|\mu|^2 + |\nu|^2 - 2\mu\nu^*)\exp(-2\kappa t_3)}, \tag{B9a}$$

$$\mho_{B,eg}(\mu,\nu,t_3) = \left(-\frac{i}{2} + ie^{-2\gamma_0 t_1}\right) \exp[-\gamma_0 t_2 + (-i\chi - \gamma_c)t_3 + \Theta(\kappa,\chi,\mu,\nu,t_3) - \frac{1}{2}(|\mu|^2 + |\nu|^2 - 2\mu\nu^* e^{-2i\chi t_3})e^{-2\kappa t_3}], \tag{B9b}$$

$$\mho_{B,ge}(\mu,\nu,t_3) = \left(\frac{i}{2} - ie^{-2\gamma_0 t_1}\right) \exp[-\gamma_0 t_2 + (i\chi - \gamma_c)t_3 + \Theta(\kappa,-\chi,\mu,\nu,t_3) - \frac{1}{2}(|\mu|^2 + |\nu|^2 - 2\mu\nu^* e^{2i\chi t_3})e^{-2\kappa t_3}], \tag{B9c}$$

$$\mho_{B,gg}(\mu,\nu,t_3) = \left(1 - \frac{1}{2} e^{-2\gamma t_2}\right) e^{\Theta(\kappa,0,\mu,\nu,t_3) - \frac{1}{2}(|\mu|^2 + |\nu|^2 - 2\mu\nu^*)\exp(-2\kappa t_3)} + 2\gamma_c \int_0^{t_3} dt \frac{1}{2} e^{-2\gamma_0 t_2 - 2\gamma_c t + \Theta(\kappa,0,\mu,\nu,t) - \frac{1}{2}(|\mu|^2 + |\nu|^2 - 2\mu\nu^*)\exp(-2\kappa t)}. \tag{B9d}$$

4. Decoherence right before final measurements and the correlation function

We now consider the last measurement process for both parties. Atom A experiences spontaneous emission for time $t_5 - t_3$ with rate γ', and then atomic displacement operation $\hat{D}_A^\dagger(-e^{-i\phi}\pi/4)$ is applied. After the displacement operation, atom A evolves again under the spontaneous emission for time t_1 with rate γ_0. We define superoperator $\hat{\mathcal{X}}$ to describe this process as

$$\hat{\mathcal{X}}_A(\gamma',\gamma_0,t_5 - t_3,t_1,\phi)[\hat{\rho}_A] = \hat{S}_A(\gamma_0,t_1)[\hat{D}_A^\dagger(-e^{-i\phi}\pi/4)\{\hat{S}_A(\gamma',t_5 - t_3)[\hat{\rho}_A]\}\hat{D}_A(-e^{-i\phi}\pi/4)]. \tag{B10}$$

Atom B undergoes spontaneous emission for time t_2 with rate γ_0, and displacement operation $\hat{D}_B^\dagger(-\pi/4)$ is applied. It then experiences spontaneous emission for time t_1 with rate γ_0 just before the final measurement. This process can be expressed as

$$\hat{\mathcal{X}}_B(\gamma_0,\gamma_0,t_2,t_1,0)[\hat{\rho}_B] = \hat{S}_B(\gamma_0,t_1)[\hat{D}_B^\dagger(-\pi/4)\{\hat{S}_B(\gamma_0,t_2)[\hat{\rho}_B]\}\hat{D}_B(-\pi/4)]. \tag{B11}$$

The final density operator used to obtain the correlation function is then obtained using state $\hat{\rho}_{AB}$ in Eq. (B7) with $\hat{\mathcal{X}}_A$ and $\hat{\mathcal{X}}_B$ as

$$\hat{\rho}_{AB}^{\text{final}} = \hat{\mathcal{X}}_A(\gamma',\gamma_0,t_5 - t_3,t_1,\phi) \otimes \hat{\mathcal{X}}_B(\gamma_0,\gamma_0,t_2,t_1,0)[\hat{\rho}_{AB}]. \tag{B12}$$

The correlation function is obtained as the expectation value of dichotomic measurements (4) performed by both the parties:

$$E(\phi,\beta,t_1,t_2,t_3,t_4,t_5)$$
$$= \text{Tr}[\hat{\rho}_{AB}^{\text{final}} \hat{\Gamma}_A \otimes \hat{\Gamma}_B] = \frac{1}{2} e^{-2\gamma_0 t_2 - 2\gamma_c t_3 - 2\gamma' t_4}(e^{-2\gamma_0 t_1} - 1)(1 - e^{-2\gamma' t_3} + e^{-2\gamma' t_5})\xi_B(\Lambda_1,\Lambda_1,t_3) + \mathcal{Z}\xi_B(\Lambda_1,\Lambda_2,t_3) + \mathcal{Z}^*\xi_B(\Lambda_2,\Lambda_1,t_3)$$
$$+ (e^{-2\gamma_0 t_1} - 1)\{\left(1 - \frac{1}{2} e^{-2\gamma_0 t_2}\right)\xi_B(\Lambda_2,\Lambda_2,t_3) + 2\gamma_c \int_0^{t_3} dt \frac{1}{2} e^{-2\gamma_0 t_2 - 2\gamma_c t}\xi_B(i\alpha e^{-rt - \kappa t_4} - \beta, i\alpha e^{-rt - \kappa t_4} - \beta, t_3)$$
$$+ 2\gamma' \int_0^{t_4} dt \frac{1}{2} e^{-2\gamma_0 t_2 - 2\gamma_c t_3 - 2\gamma' t}\xi_B(i\alpha e^{-rt_3 - \kappa t} - \beta, i\alpha e^{-rt_3 - \kappa t} - \beta, t_3)\}, \tag{B13}$$

where

$$\xi_B(\mu,\nu,t_3) = [\mho_{B,ee}(\mu,\nu,t_3) + \mho_{B,gg}(\mu,\nu,t_3)](e^{-2\gamma_0 t_1} - 1) + [\mho_{B,eg}(\mu,\nu,t_3) + \mho_{B,ge}(\mu,\nu,t_3)]e^{-\gamma_0 t_5 - 2\gamma_0 t_1}, \tag{B14}$$

$$\mathcal{Z} = \left(-\frac{i}{2} + ie^{-2\gamma_0 t_1}\right) e^{-\gamma_0(t_2 + 2t_1) + (-i\chi - \gamma_c)t_3 - \gamma'(t_4 + t_5) + \Theta(\kappa,\chi,\alpha,\alpha,t_3) + \Theta(\kappa,0,\alpha e^{-rt_3}, \alpha e^{-r^* t_3}, t_4) - 2ie^{-\kappa(t_4 + t_3)}\sin(\chi t_3)\text{Im}(\alpha^*\beta) + i\phi},$$

$\Lambda_1 = i\alpha e^{-rt_3 - \kappa t_4} - \beta$ and $\Lambda_2 = i\alpha e^{-r^* t_3 - \kappa t_4} - \beta$. Using this correlation function, one can eventually construct the Bell function using Eq. (3).

[1] A. Einstein, B. Podolsky, and N. Rosen, Phys. Rev. **47**, 777 (1935).

[2] J. S. Bell, Physics **1**, 195 (1964).

[3] J. F. Clauser, M. A. Horne, A. Shimony, and R. A. Holt, Phys. Rev. Lett. **23**, 880 (1969).

[4] S. J. Freedman and J. F. Clauser, Phys. Rev. Lett. **28**, 938 (1972).

[5] A. Aspect, P. Grangier, and G. Roger, Phys. Rev. Lett. **47**, 460 (1981).

[6] W. Tittel, J. Brendel, H. Zbinden, and N. Gisin, Phys. Rev. Lett. **81**, 3563 (1998).

[7] G. Weihs, T. Jennewein, C. Simon, H. Weinfurter, and A. Zeilinger, Phys. Rev. Lett. **81**, 5039 (1998).

[8] P. M. Pearle, Phys. Rev. D **2**, 1418 (1970).

[9] M. A. Rowe, D. Kielpinski, V. Meyer, C. A. Sackett, W. M. Itano, C. Monroe, and D. J. Wineland, Nature **409**, 791 (2001).

[10] D. N. Matsukevich, P. Maunz, D. L. Moehring, S. Olmschenk, and C. Monroe, Phys. Rev. Lett. **100**, 150404 (2008).

[11] J. S. Bell, J. Phys. C **2**, 41 (1981).

[12] M. S. Kim and J. Lee, Phys. Rev. A **61**, 042102 (2000).

[13] P. Milman, A. Auffeves, F. Yamaguchi, M. Brune, J. M. Raimond, and S. Haroche, Eur. Phys. J. D **32**, 233 (2005).

[14] C. Simon and W. T. M. Irvine, Phys. Rev. Lett. **91**, 110405 (2003).

[15] J. Volz, M. Weber, D. Schlenk, W. Rosenfeld, J. Vrana, K. Saucke, C. Kurtsiefer, and H. Weinfurter, Phys. Rev. Lett. **96**, 030404 (2006).

[16] N. Brunner, N. Gisin, V. Scarani, and C. Simon, Phys. Rev. Lett. **98**, 220403 (2007).

[17] N. Sangouard, J.-D. Bancal, N. Gisin, W. Rosenfeld, P. Sekatski, M. Weber, and H. Weinfurter, Phys. Rev. A **84**, 052122 (2011).

[18] N. Spagnolo, C. Vitelli, M. Paternostro, F. De Martini, and F. Sciarrino, Phys. Rev. A **84**, 032102 (2011).

[19] D. L. Moehring, M. J. Madsen, B. B. Blinov, and C. Monroe, Phys. Rev. Lett. **93**, 090410 (2004).

[20] K. Wódkiewicz, New J. Phys. **2**, 21 (2000).

[21] E. Schrödinger, Naturwissenschaften **23**, 823 (1935).

[22] M. Brune, E. Hagley, J. Dreyer, X. Maître, A. Maali, C. Wunderlich, J. M. Raimond, and S. Haroche, Phys. Rev. Lett. **77**, 4887 (1996).

[23] C. Guerlin, J. Bernu, S. Deleglise, C. Sayrin, S. Gleyzes, S. Kuhr, M. Brune, J.-M. Raimond, and S. Haroche, Nature **448**, 889 (2007).

[24] S. Deleglise, I. Dotsenko, C. Sayrin, J. Bernu, M. Brune, J.-M. Raimond, and S. Haroche, Nature **455**, 510 (2008).

[25] H. Jeong and T. C. Ralph, Phys. Rev. Lett. **97**, 100401 (2006); Phys. Rev. A **76**, 042103 (2007).

[26] F. De Martini, F. Sciarrino, and C. Vitelli, Phys. Rev. Lett. **100**, 253601 (2008).

[27] N. Spagnolo, C. Vitelli, F. Sciarrino, and F. De Martini, Phys. Rev. A **82**, 052101 (2010).

[28] W. J. Munro, G. J. Milburn, and B. C. Sanders, Phys. Rev. A **62**, 052108 (2000).

[29] D. Wilson, H. Jeong, and M. S. Kim, J. Mod. Opt., Special Issue for QEP **49**, 851 (2002).

[30] H. Jeong, W. Son, M. S. Kim, D. Ahn, and Č. Brukner, Phys. Rev. A **67**, 012106 (2003).

[31] H. Jeong and N. B. An, Phys. Rev. A **74**, 022104 (2006).

[32] M. Stobińska, H. Jeong, and T. C. Ralph, Phys. Rev. A **75**, 052105 (2007).

[33] H. Jeong, Phys. Rev. A **78**, 042101 (2008).

[34] H. Jeong, M. Paternostro, and T. C. Ralph, Phys. Rev. Lett. **102**, 060403 (2009).

[35] C. C. Gerry, A. Benmoussa, E. E. Hach, and J. Albert, Phys. Rev. A **79**, 022111 (2009).

[36] C.-W. Lee and H. Jeong, Phys. Rev. A **80**, 052105 (2009).

[37] B. S. Cirel'son, Lett. Math. Phys. **4**, 93 (1980).

[38] S. Haroche and J. Raimond, *Exploring the Quantum, Atoms, Cavities, and Photons* (Oxford University Press, New York, 2006).

[39] H. Yuen and J. Shapiro, IEEE Trans. Inf. Theory **26**, 78 (1980).

[40] R. A. Campos, B. E. A. Saleh, and M. C. Teich, Phys. Rev. A **40**, 1371 (1989).

[41] W. H. Press, B. P. Flannery, S. A. Teukolsky, and W. T. Vetterling, *Numerical Recipes* (Cambridge University Press, Cambridge, 1988).

[42] N. Gisin and B. Gisin, Phys. Lett. A **260**, 323 (1999).

[43] M. Brune, S. Haroche, J. M. Raimond, L. Davidovich, and N. Zagury, Phys. Rev. A **45**, 5193 (1992).

[44] L. Davidovich, M. Brune, J. M. Raimond, and S. Haroche, Phys. Rev. A **53**, 1295 (1996).

[45] J. M. Raimond, M. Brune, and S. Haroche, Rev. Mod. Phys. **73**, 565 (2001).

[46] P. Nussenzveig, F. Bernardot, M. Brune, J. Hare, J. M. Raimond, S. Haroche, and W. Gawlik, Phys. Rev. A **48**, 3991 (1993).

[47] B.-G. Englert, N. Sterpi, and H. Walther, Opt. Commun. **100**, 526 (1993).

[48] R. G. Hulet, E. S. Hilfer, and D. Kleppner, Phys. Rev. Lett. **55**, 2137 (1985).

[49] K. Kakazu and Y. S. Kim, Prog. Theor. Phys. **96**, 883 (1996).

[50] M. Wilkens, Z. Bialynicka-Birula, and P. Meystre, Phys. Rev. A **45**, 477 (1992).

[51] J. G. Peixoto de Faria and M. C. Nemes, Phys. Rev. A **59**, 3918 (1999).

[52] X. Zhou, C. Sayrin, S. Deléglise, J. Bernu, C. Guerlin, S. Gleyzes, S. Kuhr, I. Dotsenko, J.-M. Raimond, and S. Haroche [http://www.cqed.org/IMG/pdf/2009-LKB-AERES-Techniques_low.pdf].

[53] S. Kuhr, S. Gleyzes, C. Guerlin, J. Bernu, U. B. Hoff, S. Deléglise, S. Osnaghi, M. Brune, J.-M. Raimond, S. Haroche, E. Jacques, P. Bosland, and B. Visentin, Appl. Phys. Lett. **90**, 164101 (2007).

[54] P. Maioli, T. Meunier, S. Gleyzes, A. Auffeves, G. Nogues, M. Brune, J. M. Raimond, and S. Haroche, Phys. Rev. Lett. **94**, 113601 (2005).

[55] S. J. D. Phoenix, Phys. Rev. A **41**, 5132 (1990).

[56] H. Moya-Cessa, Phys. Rep. **432**, 1 (2006).

[57] W. Witschel, Int. J. Quantum Chem. **20**, 1233 (1981).